Contents

List of Figures

List of Tables

1 Potential Scattering

Scattering calculations have been performed for a projectile, with charge z_{proj}, scattering off a structure-less potential (equivalently - a one-state target) of the form

$$V(r) = z_{\text{proj}}\left(1 + \frac{1}{r}\right)e^{-2r}. \tag{1}$$

In these scattering calculations, the following parameters were constant: $r_{\max} = 200$, $\text{dr} = 0.001$ and $\ell_{\min} = 0$. Two sets of calculations were performed:

1. With $\ell_{\max} = 5$; for $z_{\text{proj}} \in \{-1, +1\}$, for $E_{\text{proj}} \in \{E_k = \alpha + \beta k^2\}_{k=1}^{20}$ with α, β such that $E_1 = 0.1\,\text{eV}$ and $E_{20} = 50.0\,\text{eV}$, the calculation was performed, and the ICS and DCS curves extracted.

2. With $z_{\text{proj}} = -1$, and $E_{\text{proj}} = 25.0\,\text{eV}$; for $\ell \in \{0, \ldots, 9\}$, the calculation was performed, and the ICS and DCS curves extracted.

1.1 ICS Curves

The total and partial Integrated-Cross-Section (ICS) curves, extracted from the first set of calculations, are shown for an electron and positron projectile in Figure 1 and Figure 2 respectively.

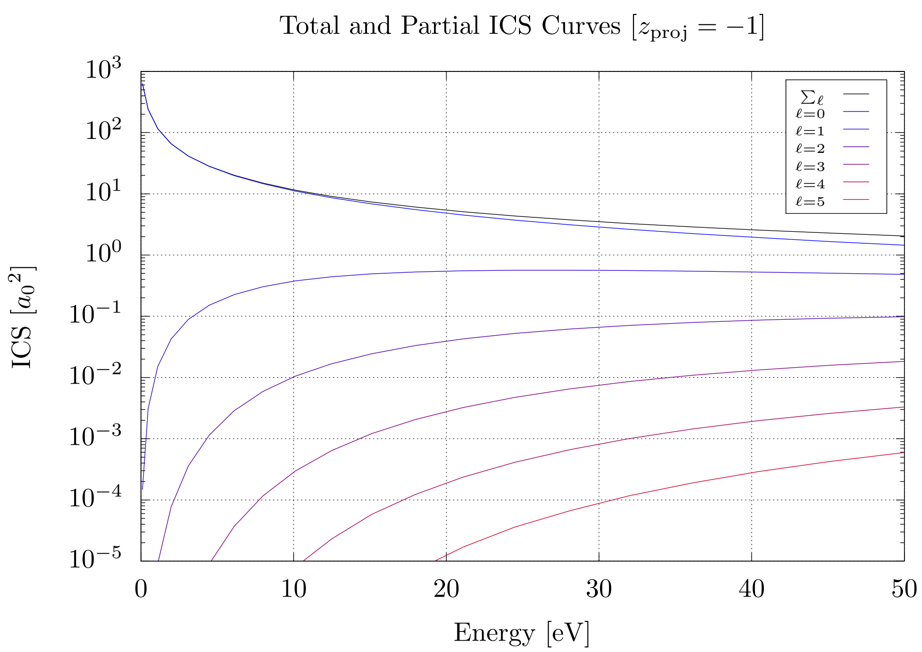

Figure 1: The total ICS curve (shown in black) and the partial ICS curves (shown in blue-to-red) are presented, across projectile energies $0.1\,\text{eV}$ *to* $50\,\text{eV}$*, for an electron projectile, with* $\ell_{\min} = 0$ *and* $\ell_{\max} = 5$*. Note that the y-axis is presented in log-scale.*

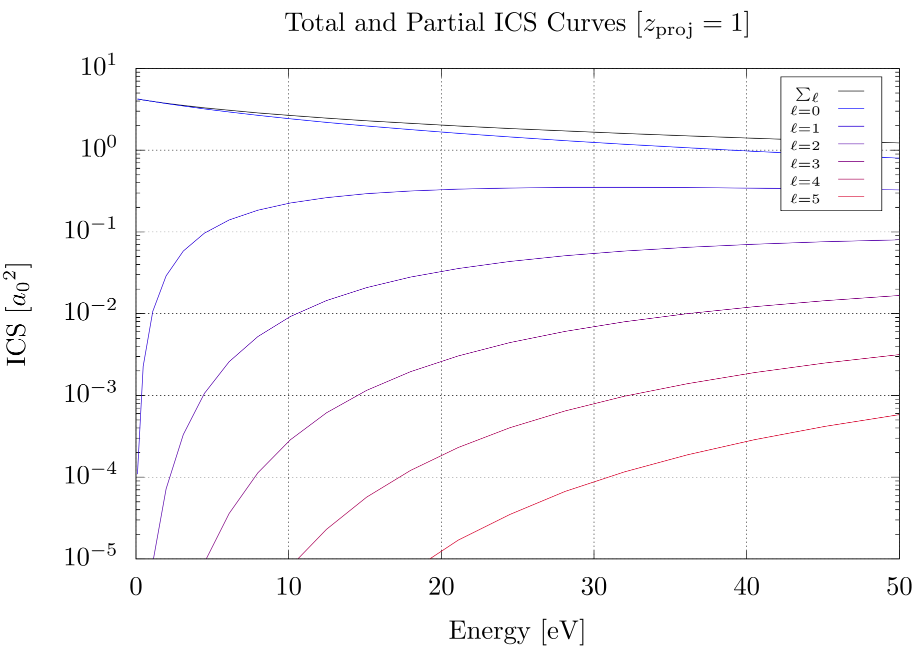

Figure 2: The total ICS curve (shown in black) and the partial ICS curves (shown in blue-to-red) are presented, across projectile energies $0.1\,\text{eV}$ *to* $50\,\text{eV}$*, for a positron projectile, with* $\ell_{\text{min}} = 0$ *and* $\ell_{\text{max}} = 5$*. Note that the y-axis is presented in log-scale.*

1.2 DCS Curves

The Differential-Cross-Section (DCS) curves, extracted from the first set of calculations, are shown for an electron and positron projectile in Figure 3 and Figure 4 respectively.

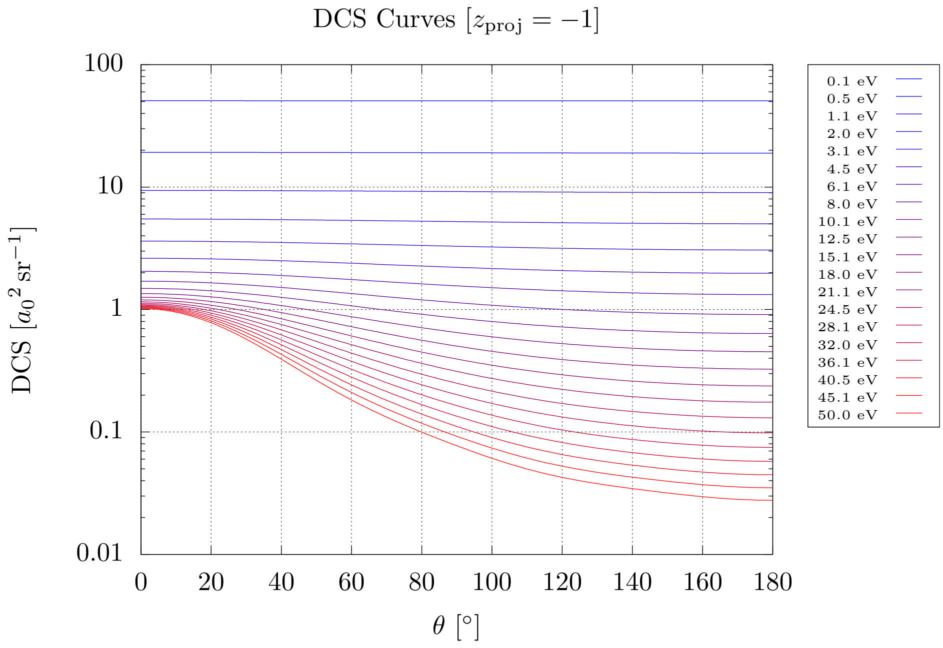

Figure 3: The DCS curves (shown in blue-to-red) are presented, across scattering angles $0°$ to $180°$, for an electron projectile, with projectile energies ranging across $0.1\,\text{eV}$ to $50\,\text{eV}$, and with $\ell_{\min} = 0$ and $\ell_{\max} = 5$. Note that the y-axis is presented in log-scale.

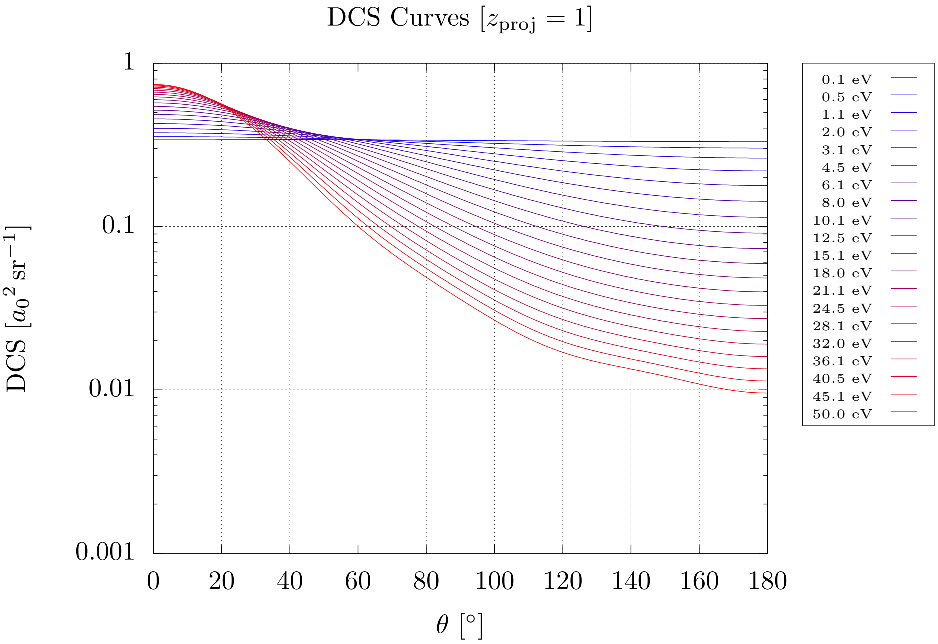

Figure 4: The DCS curves (shown in blue-to-red) are presented, across scattering angles 0° *to* 180°*, for a positron projectile, with projectile energies ranging across* $0.1\,\text{eV}$ *to* $50\,\text{eV}$*, and with* $\ell_{\text{min}} = 0$ *and* $\ell_{\text{max}} = 5$*. Note that the y-axis is presented in log-scale.*

1.3 DCS Curve Convergence

The Differential-Cross-Section (DCS) curves, extracted from the second set of calculations, are shown in Figure 5.

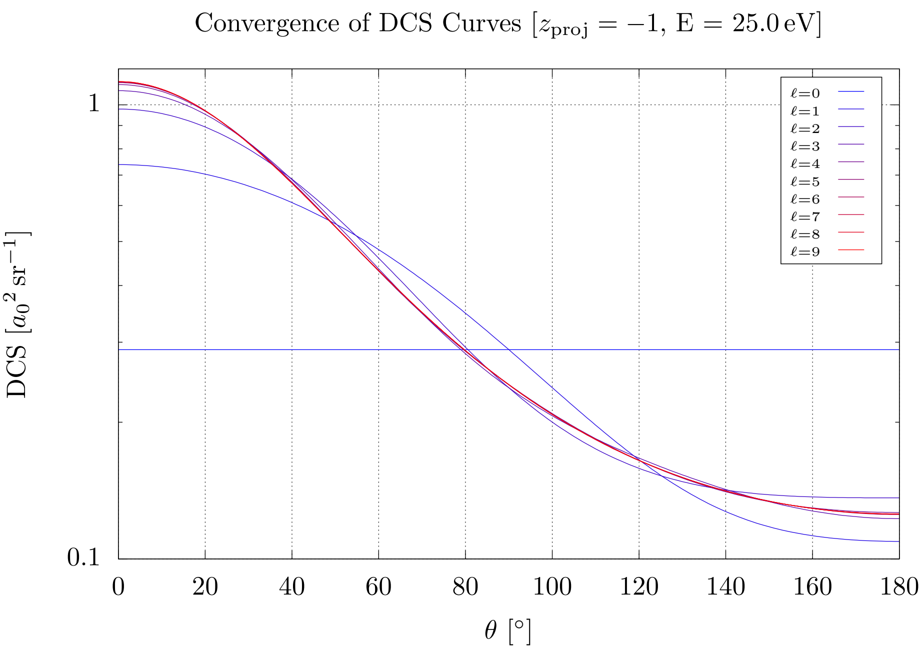

Figure 5: The DCS curves (shown in blue-to-red) are presented, across scattering angles $0°$ to $180°$, for an electron projectile, with projectile energy $E = 25.0\,\text{eV}$, and $\ell_{\min} = 0$, with $\ell_{\max}$ ranging across 0 to 9. Note that the y-axis is presented in log-scale.

It can be seen that the DCS converges rather quickly for this projectile energy of $25.0\,\text{eV}$. A point of interest is that the DCS curve, for $\ell_{\max} = 0$, is constant. This is a consequence of the behaviour of the zeroth-order Legendre polynomials $P_\ell(\cos\theta)$, for which $P_0(\cos\theta) = 1$. To see this, note that the differential cross section, for this scattering calculation, is of the form

$$\frac{\mathrm{d}\sigma}{\mathrm{d}\Omega}(\theta) = |f(\mathbf{k}_f, \mathbf{k}_i)|^2$$

where $\mathbf{k}_f$ is such that $k_f = k_i$, and where $\cos\theta = \hat{\mathbf{k}}_f \cdot \hat{\mathbf{k}}_i$, with the scattering amplitude being of the form

$$f(\mathbf{k}_f, \mathbf{k}_i) = -\frac{\pi}{k_i^2} \sum_{\ell=\ell_{\min}}^{\ell_{\max}} (2\ell+1) T_\ell(k_i, k_i) P_\ell(\cos\theta).$$

Hence, where $\ell_{\min} = \ell_{\max} = 0$, we have that

$$f(\mathbf{k}_f, \mathbf{k}_i) = -\frac{\pi}{k_i^2} \sum_{\ell=0}^{0} T_0(k_i, k_i) P_0(\cos\theta) = -\frac{\pi}{k_i^2} T_0(k_i, k_i)$$

whence

$$\frac{\mathrm{d}\sigma}{\mathrm{d}\Omega}(\theta) = \frac{\pi^2}{k_i^4} |T_0(k_i, k_i)|^2$$

demonstrating the constant behaviour of the DCS curve for $\ell_{\max} = 0$.

2 Derivation

The 3D Lippmann-Schwinger equation is of the form

$$\langle \boldsymbol{k}_f | T | \boldsymbol{k}_i \rangle = \langle \boldsymbol{k}_f | V | \boldsymbol{k}_i \rangle + \int \mathrm{d}\boldsymbol{k}\, \frac{\langle \boldsymbol{k}_f | V | \boldsymbol{k} \rangle \; \langle \boldsymbol{k} | T | \boldsymbol{k}_i \rangle}{E + \mathrm{i}0 - \frac{1}{2}k^2}. \tag{2}$$

We note that the partial-wave expansion of the T-matrix is of the form

$$\langle \boldsymbol{k}_f | T | \boldsymbol{k}_i \rangle = \frac{1}{k_f k_i} \sum_{\ell,m} T_\ell(k_f, k_i) Y_{\ell m}(\hat{\boldsymbol{k}}_f) Y^*_{\ell m}(\hat{\boldsymbol{k}}_i) \tag{3}$$

and similarily so for the partial-wave expansion of the V-matrix,

$$\langle \boldsymbol{k}_f | V | \boldsymbol{k}_i \rangle = \frac{1}{k_f k_i} \sum_{\ell,m} V_\ell(k_f, k_i) Y_{\ell m}(\hat{\boldsymbol{k}}_f) Y^*_{\ell m}(\hat{\boldsymbol{k}}_i). \tag{4}$$

Replacing the left hand side of Equation 2 with the partial-wave expansion of the T-matrix, we have that

$$\mathrm{LHS} = \frac{1}{k_f k_i} \sum_{\ell,m} T_\ell(k_f, k_i) Y_{\ell m}(\hat{\boldsymbol{k}}_f) Y^*_{\ell m}(\hat{\boldsymbol{k}}_i)$$

while substituting in the partial-wave expansions into the right hand side of Equation 2, we have that

$$\begin{aligned}
\mathrm{RHS} &= \frac{1}{k_f k_i} \sum_{\ell,m} V_\ell(k_f, k_i) Y_{\ell m}(\hat{\boldsymbol{k}}_f) Y^*_{\ell m}(\hat{\boldsymbol{k}}_i) \\
&\quad + \int \mathrm{d}\boldsymbol{k}\, \frac{1}{E + \mathrm{i}0 - \frac{1}{2}k^2} \left(\frac{1}{k_f k} \sum_{\ell,m} V_\ell(k_f, k) Y_{\ell m}(\hat{\boldsymbol{k}}_f) Y^*_{\ell m}(\hat{\boldsymbol{k}}) \right) \left(\frac{1}{k k_i} \sum_{\ell',m'} T_{\ell'}(k, k_i) Y_{\ell' m'}(\hat{\boldsymbol{k}}) Y^*_{\ell' m'}(\hat{\boldsymbol{k}}_i) \right) \\
&= \frac{1}{k_f k_i} \sum_{\ell,m} V_\ell(k_f, k_i) Y_{\ell m}(\hat{\boldsymbol{k}}_f) Y^*_{\ell m}(\hat{\boldsymbol{k}}_i) \\
&\quad + \frac{1}{k_f k_i} \sum_{\ell,m} \sum_{\ell',m'} Y_{\ell m}(\hat{\boldsymbol{k}}_f) Y^*_{\ell' m'}(\hat{\boldsymbol{k}}_i) \int \mathrm{d}\boldsymbol{k}\, \frac{1}{k^2} \frac{V_\ell(k_f, k) T_{\ell'}(k, k_i) Y^*_{\ell m}(\hat{\boldsymbol{k}}) Y_{\ell' m'}(\hat{\boldsymbol{k}})}{E + \mathrm{i}0 - \frac{1}{2}k^2} \\
&= \frac{1}{k_f k_i} \sum_{\ell,m} \Bigg(V_\ell(k_f, k_i) Y_{\ell m}(\hat{\boldsymbol{k}}_f) Y^*_{\ell m}(\hat{\boldsymbol{k}}_i) \\
&\quad + \sum_{\ell',m'} Y_{\ell m}(\hat{\boldsymbol{k}}_f) Y^*_{\ell' m'}(\hat{\boldsymbol{k}}_i) \int \mathrm{d}k\, \frac{V_\ell(k_f, k) T_{\ell'}(k, k_i)}{E + \mathrm{i}0 - \frac{1}{2}k^2} \int \mathrm{d}\hat{\boldsymbol{k}}\, Y^*_{\ell m}(\hat{\boldsymbol{k}}) Y_{\ell' m'}(\hat{\boldsymbol{k}}) \Bigg) \\
&= \frac{1}{k_f k_i} \sum_{\ell,m} \left(V_\ell(k_f, k_i) + \int \mathrm{d}k\, \frac{V_\ell(k_f, k) T_\ell(k, k_i)}{E + \mathrm{i}0 - \frac{1}{2}k^2} \right) Y_{\ell m}(\hat{\boldsymbol{k}}_f) Y^*_{\ell m}(\hat{\boldsymbol{k}}_i)
\end{aligned}$$

where other than simple algebraic re-arrangment, we have utilised the orthogonality of the spherical harmonics to reduce the sum over ℓ', m'. It then follows, on subtracting one side from the other, that

$$\mathrm{LHS} - \mathrm{RHS} = \frac{1}{k_f k_i} \sum_{\ell,m} \left(T_\ell(k_f, k_i) - V_\ell(k_f, k_i) + \int \mathrm{d}k\, \frac{V_\ell(k_f, k) T_\ell(k, k_i)}{E + \mathrm{i}0 - \frac{1}{2}k^2} \right) Y_{\ell m}(\hat{\boldsymbol{k}}_f) Y^*_{\ell m}(\hat{\boldsymbol{k}}_i)$$

which is zero if and only if the term inside the sum is zero for all ℓ, m; that is to say, that we must have

$$T_\ell(k_f, k_i) = V_\ell(k_f, k_i) + \int \mathrm{d}k\, \frac{V_\ell(k_f, k) T_\ell(k, k_i)}{E + \mathrm{i}0 - \frac{1}{2}k^2} \tag{5}$$

whence we have the partial-wave Lippmann-Schwinger equation.

3 Dimensional Analysis

We note that the partial-wave T-matrix elements are linearly added with the partial-wave V-matrix elements in Equation 5, and so they must have the same units; that is, $[T_\ell(k_f, k_i)] = [V_\ell(k_f, k_i)]$. We note also that we are working in units where $[E] = [k^2]$, with $[k] = L^{-1}$. In dimensional terms, the partial-wave Lippmann-Schwinger equation is of the form

$$[T_\ell(k_f, k_i)] - [V_\ell(k_f, k_i)] = \left[\int \mathrm{d}k \, \frac{V_\ell(k_f, k) T_\ell(k, k_i)}{E - \frac{1}{2}k^2}\right] = [V_\ell(k_f, k)][T_\ell(k, k_i)]\left[\int \mathrm{d}k \, \frac{1}{E - \frac{1}{2}k^2}\right]$$

where we note that

$$\left[\int \mathrm{d}k \, \frac{1}{E - \frac{1}{2}k^2}\right] = L^2 \left[\int \mathrm{d}k\right] = L.$$

It therefore follows that the units of the partial-wave T-matrix elements must satisfy

$$[T_\ell(k_f, k_i)] = [T_\ell(k, k_i)]^2 L$$

whence we have that $[T_\ell(k_f, k_i)] = L^{-1}$. To verify this, note that the partial-wave cross sections, σ_ℓ, have units $[\sigma_\ell] = L^2$, and are defined by the expression

$$\sigma_\ell = \frac{4\pi^3}{k_i^4}(2\ell + 1)|T_\ell(k_f, k_i)|^2$$

which, written in dimensional terms, is of the form

$$[\sigma_\ell] = \frac{1}{[k_i]^4}[T_\ell(k_f, k_i)]^2 = L^4 L^{-2} = L^2$$

yielding the appropriate units as required.